Low Sintering Temperature and Electrical Properties of Samarium-Doped Ceria

E. C. C. Souza[a] and E. N. S. Muccillo[a]

[a]Center of Materials Science and Technology, Energy and Nuclear Research Institute, S. Paulo, 05508-000, SP, Brazil

$Ce_{0.8}Sm_{0.2}O_{1.95}$ solid electrolyte was synthesized by a modified homogeneous precipitation method aiming optimizing its densification behavior and electrical conductivity. Nanoparticles with 3 to 8 nm in diameter were obtained after calcination at 450 and 700ºC respectively. The linear shrinkage of powder compacts shows an endset temperature around 1200ºC with maximum shrinkage rate at 1000ºC. High relative density values (~ 93%) were obtained for pellets prepared from mixed solvents at only 1150ºC. The electrical conductivity of both grains and grain boundaries exhibits a considerable dependence on the type of alcohol used as solvent and on the residual porosity.

Introduction

Rare-earth doped cerium oxide ceramics have been extensively studied over the last years to be used as solid electrolyte in intermediate temperature (500-700ºC) solid oxide fuel cells (1,2). One of the main advantages for the use of doped-ceria ceramics instead of the well-known yttria-stabilized zirconia is the possibility of reduction in the operation temperature of this type of device, and thereby reduction of production costs (3).

Several efforts have been devoted to the synthesis of doped-ceria ceramics with high sinterability to improve the densification process and to optimize the ionic conductivity. A number of methods of synthesis have been used for this purpose. Chen and Chen (4) demonstrated the advantages of the homogeneous precipitation over the conventional oxalate or hydroxide coprecipitation methods. The homogeneous precipitation method has been previously applied for the preparation of doped ceria solid solutions (5-7) resulting in the production of nanoparticles with less than 25 nm. In this kinetically controlled method of synthesis, high chemical homogeneity of the powder particles along with a sharp distribution of particle sizes is expected to occur.

It was recently reported by the authors, the synthesis of $Ce_{1-x}Sm_xO_{2-\delta}$ ($0 \leq x \leq 30$) by the modified homogeneous precipitation method using alcoholic solvents (8). It was shown that the use of a low dielectric constant solvent allowed for obtaining single-crystalline samaria-doped ceria nanoparticles without the thermal decomposition step. Powders prepared with different mixtures of water/alcohol exhibited different densification behaviors. These differences were explained as a consequence of a varying degree of agglomeration of the powder particles. The ionic conductivity of sintered pellets was improved when compared to that of specimens prepared by the conventional solid state synthesis method. In this work, further characterization of $Ce_{0.8}Sm_{0.2}O_{1.95}$ prepared by this modified method will be focused, with special attention to the electrical conductivity.

Experimental

Sample Preparation

Cerium nitrate hexahydrate ($Ce(NO_3)_3.6H_2O$, 99.99, Aldrich), samarium nitrate hexahydrate ($Sm(NO_3)_3.6H_2O$, 99.9%, Strem. Chem.), and hexamethylenetetramine ($(CH_2)_6N_4$, 99%, Alfa Aesar) were used as starting materials. $Ce_{0.8}Sm_{0.2}O_{1.95}$ solid electrolyte was prepared by the homogeneous precipitation method using a mixture of water/alcohol (50% v/v.) as solvent. In this study isopropyl (*i*-PrOH) and ethyl (EtOH) alcohols were used due to their high solubility in water. A full description of the method and of the parameters involved in the synthesis process may be found elsewhere (8). The precipitate was dried in an oven at 70ºC for 24 h. Cylindrical pellets were prepared after calcination at 700ºC by uniaxial pressing at 98 MPa followed by sintering in air at several dwell temperatures and soaking times. $Ce_{0.8}Sm_{0.2}O_{1.95}$ pellets were also prepared with a commercial powder (SDC-20, Fuel Cell Materials) for comparison purposes.

Sample Characterization

The actual Sm^{3+} content was determined from energy dispersive spectroscopy, EDS, analysis on sintered pellets. The morphology of powder particles was examined by high resolution transmission electron microscopy (HRTEM, JEM 3010 URP). Apparent sintered density values were obtained from water immersion method. The linear shrinkage behavior of some compacts were evaluated by dilatometry (Labsys, Setaram) from room temperature up to 1400ºC with a heating rate of $5ºC.min^{-1}$ in stagnant atmosphere of synthetic air. Electrical conductivity measurements were carried out by impedance spectroscopy (HP4192A) in the 5 Hz -13 MHz frequency range. Silver paste was applied onto large surfaces of the pellets and cured at 400ºC to act as electrode material. The electrical conductivity was calculated from measured resistance value and normalized for sample dimension. No correction for porosity was applied.

Results and Discussion

Chemical and microstructure characterizations

Previous studies (1,9) on the composition-dependence of the electrical conductivity of samaria-doped ceria have shown that a maximum in the isothermal conductivity curve was obtained at 20 mol% $SmO_{1.5}$. Then, in order to obtain an as much as possible exact stoichiometry in the prepared material, powders containing different amounts of $SmO_{1.5}$ were synthesized and used to obtain a calibration curve for determining the actual Sm^{3+} content using energy dispersive spectroscopy analysis. This calibration curve for sintered pellets is shown in Fig. 1.

This result shows that the precipitation of Ce^{3+} and Sm^{3+} is not quantitative, as expected, due to the different rates of hydrolysis of both cations, and may explain some differences observed in published electrical conductivity data. This calibration curve was used to obtain stoichiometric $Ce_{0.8}Sm_{0.2}O_{1.9}$.

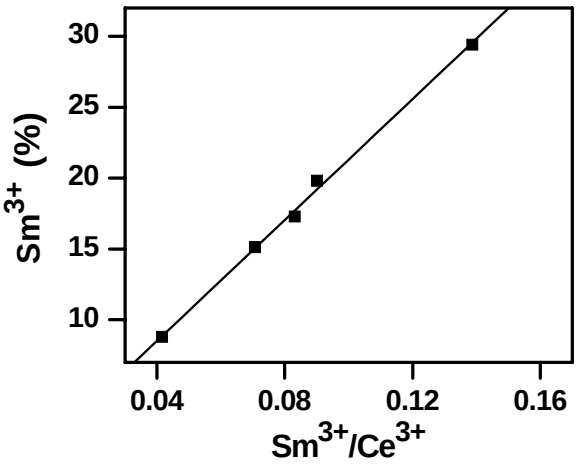

Figure 1. Relationship between the Sm^{3+}/Ce^{3+} added and the Sm^{3+} content (at.%) in sintered pellets.

Fig. 2 shows a HRTEM micrograph of the as-prepared $Ce_{0.8}Sm_{0.2}O_{1.95}$ powder before calcination.

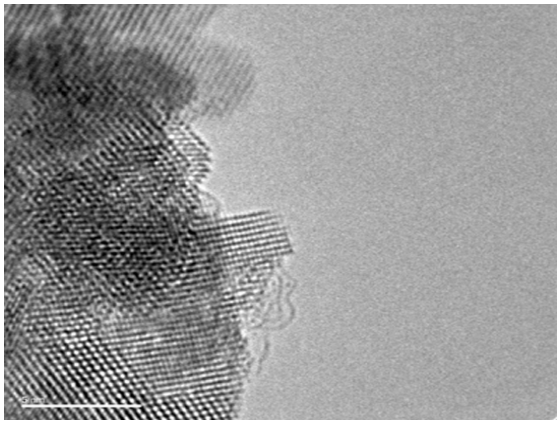

Figure 2. HRTEM of the as-prepared powder. Bar length = 5 nm.

The main microstructure features are a crowded network of nanoparticles with strong faceting. These nanoparticles exhibit lattice fringes evidencing their single crystalline nature even before any thermal treatment. The size of the produced nanoparticles after calcination at 450 and 700ºC are in the 3 to 8 nm range.

Densification behavior

Fig. 3 shows the sintered density dependence on the dwell temperature for a soaking time of 5 h. Powder compacts were prepared with powders synthesized in water/EtOH and water/*i*-PrOH mixed solvents and calcined at 700ºC for 2 h.

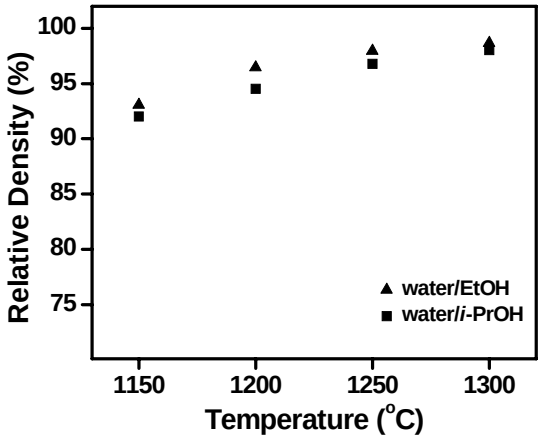

Figure 3. Relative density of powder compacts as a function of the dwell temperature. Soaking time = 5 h.

These curves show that this method of synthesis produced reactive powders that attained high density at relatively lower temperatures. At only 1150ºC the relative densities are ~ 93%. There is a small difference between the relative densities due to the use of different alcoholic solvents. However, the density curves are similar in shape.

Fig. 4 shows linear shrinkage curves of $Ce_{0.8}Sm_{0.2}O_{1.95}$ synthesized in water/EtOH solvent after calcination at 700ºC and of SDC-20 commercial powder.

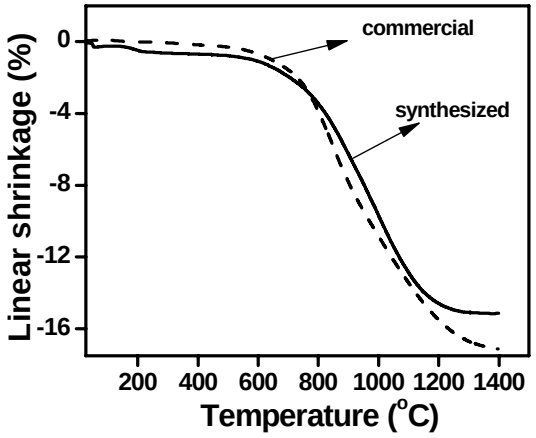

Figure 4. Linear shrinkage curves of commercial and synthesized $Ce_{0.8}Sm_{0.2}O_{1.95}$.

The synthesized powder the commercial material have a similar behavior during sintering, except for the total shrinkage that is higher in the compact prepared from commercial powder. The temperature for maximum shrinkage is about 1000ºC for the synthesized material. Total linear shrinkage is 15% and only one maximum was obtained in the derivative curve for the prepared powder indicating that a single densification mechanism occurs. In contrast, the commercial material exhibits two maxima in the derivative curve evidencing a change in the sintering behavior around 1100ºC.

Electrical conductivity

Impedance diagrams of sintered pellets consisted of two well-resolved semicircles as shown in Fig. 5 for samples prepared with synthesized powder (water/*i*-PrOH solvent) and sintered at 1150, 1200 and 1300ºC for 5 h.

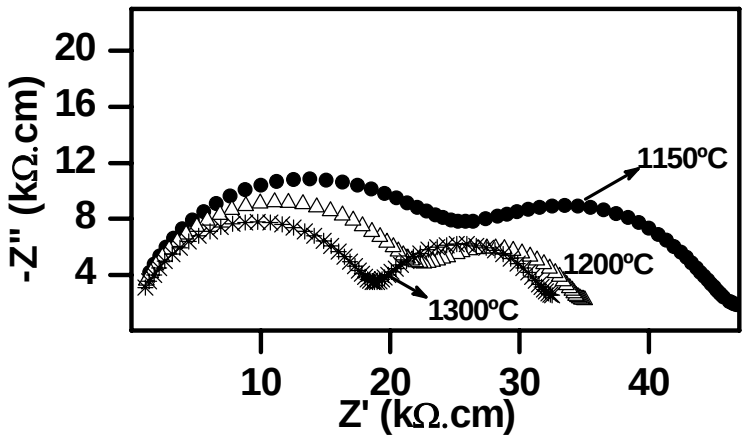

Figure 5. Impedance diagrams of pellets sintered at several dwell temperatures. Measuring temperature = 250ºC.

In these plots resistance values were normalized for sample dimensions. Increasing the sintering temperature, the overall resistivity decreases as expected due to increase in sintered density (Fig. 3).

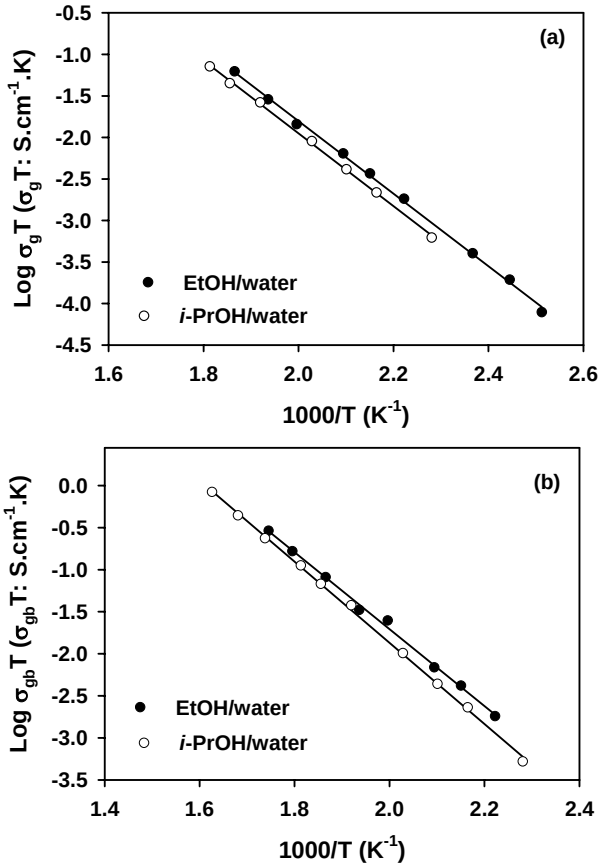

Figure 6. Arrhenius plots of the electrical conductivity of (a) grains and (b) grain boundaries for pellets sintered at 1300ºC for 5 h.

Fig. 6 shows Arrhenius plots of the electrical conductivity of grains (a) and grain boundaries (b) in pellets prepared form powders synthesized under different solvents. It can be seen that both the grain and the grain boundary conductivities of pellets prepared in water/EtOH solvent are slightly higher than those of pellets prepared with powder synthesized in water/*i*-PrOH solvent. This effect may be attributed to different impurities found in alcoholic media and to their solubility in the matrix.

In addition to minor impurities, residual porosity can also change the electrical conductivity of doped ceria ceramics. Fig. 7 shows, as an example, the Arrhenius plots of total electrical conductivity of pellets sintered at 1200 and 1300ºC for 5 h.

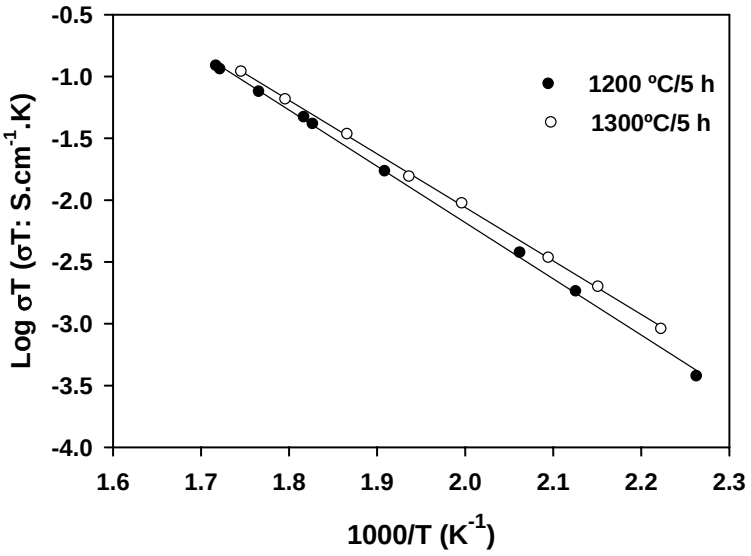

Figure 7. Arrhenius plots of total electrical conductivity of pellets sintered at different temperatures (water/EtOH solvent).

Conclusions

Acknowledgments

The authors acknowledge FAPESP, CNPq and CNEN for financial supports. E. C. C. Souza acknowledges FAPESP for the scholarship.

References

1. H. Yahiro, Y. Baba, K. Eguchi and H. Arai, *J. Electrochem. Soc*., **135**, 2077 (1988).
2. K. Eguchi, T. Setoguchi, T. Inoue and H. Arai, *Solid State Ionics*, **52**, 165 (1992).
3. B. C. H. Steele, *Solid State Ionics*, **129**, 95 (2000).
4. P.-L.Chen and I.-W. Chen, *J. Am. Ceram. Soc.*, **76**, 1577 (1993).
5. T. C. Rojas and M. Ocana, *Script. Mater*., **46**, 644 (2002).

6. J. Markmann, A. Tschope and R. Birringer, *Acta Mater*. **50**, 1433 (2002).
7. J.-G. Li, Y. Wang, T. Ikegami, T. Mori and T. Ishigaki, *Mater. Sci. Eng,*, **B121**, 54 (2005).
8. E. C. C. Souza and E. N. S. Muccillo, *J. Alloy Compd*., **xxx**, 560 (2009).
9. Z. Zhan, T.-L. Wen, H. Tu and Z.-Y. Lu, *J. Electrochem. Soc*., **148**, A427 (2001),

1. J. Doe and R. Hill, *J. Electrochem. Soc.*, **137**, 1902 (1990).
2. R. Smith, *Electrochem. Solid-State Lett.*, **1**, 1 (1998).
3. D. Warren and J. M. Woodall, in *Semiconductor Cleaning Technology/1989*, J. Ruzyllo and R. E. White, Editors, PV 90-9, p. 371, The Electrochemical Society Proceedings Series, Pennington, NJ (1990).
4. F. P. Fehlner, *Low Temperature Oxidation: The Role of Vitrous Oxides*, p. 23, Wiley Interscience, New York (1986).
5. N. J. DiNardo, in *Metallized Plastics 1*, K. L. Mittal and J. R. Susko, Editors, p. 137, Plenum Press, New York (1989).